CONF-781058--1

LA-UR -78-2658

MASTER

TITLE: DIRECT REACTION STUDIES WITH A POLARIZED TRITON BEAM

AUTHOR(S): Edward R. Flynn

SUBMITTED TO: Invited talk to be presented at the International Symposium on Direct Reactions Fukuoka, Japan, October 25-28, 1978.

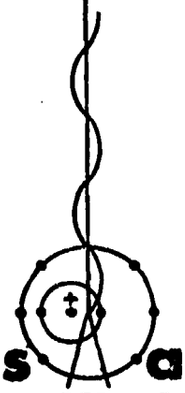

los alamos
scientific laboratory
of the University of California
LOS ALAMOS, NEW MEXICO 87545

Form No. 836
St. No. 2629
1/75

UNITED STATES
ENERGY RESEARCH AND
DEVELOPMENT ADMINISTRATION
CONTRACT W-7405-ENG. 36

DIRECT REACTION STUDIES WITH A POLARIZED TRITON BEAM

E. R. Flynn
Los Alamos Scientific Laboratory, University of California,
Los Alamos, New Mexico 87545

Abstract

A variety of direct nuclear reaction experiments have been made utilizing a polarized triton beam. Of particular interest has been the use in nuclear spectroscopy of the (t,α) and (t,d) reactions for the measurement of nuclear spins and strength factors. In addition, these reactions as well as the (t,p) and (t,t') reactions have been used to examine the role of multi-step processes in direct reactions. The analyzing power measurements appear particularly sensitive to such complex mechanisms and may be used to investigate the details of nuclear configurations of the various channels.

1. Introduction

The use of polarized beams as a spectroscopic tool is well established with numerous laboratories now possessing excellent polarized source facilities. Reactions such as $(\vec{d},p)$, $(\vec{p},d)$, and $(\vec{d},t)$ have been used extensively to establish nuclear spins through a combination of differential cross section and analyzing power measurements[1]. Inelastic scattering of protons and deuterons have also been used to investigate reaction mechanism details[2]. In recent works, the use of polarized beams has been applied to more sophisticated studies such as the role of multi-step processes in the (p,t) reaction[3]. All of these programs have shown that the additional measurement of the analyzing power based on a spin up-spin down difference adds considerably to the nuclear information obtained.

The triton has proven to be a very useful light ion for nuclear reaction studies in addition to those discussed above. These are summarized in Fig. 1. Extensive work with the (t,α), (t,d), (t,p), (t,^{3}He) and (t,t') reactions have shown the versatility of the projectile in the field of direct nuclear reactions. The triton carries spin 1/2 and isospin 1/2 with both neutrons occupying the 1s orbits. Its composite structure makes it a strongly absorbed particle which offers advantages in DWBA comparison for many reactions. In particular, the (t,d) and (t,t') are well fit by such calculations offering

TRITON PROPERTIES

General

isospin 1/2 (same as neutron)
charge one
strongly absorbed
weakly bound
neutron pair in s-orbital

Reactions:

(t,d) Principally surface so well fit by DWBA
Higher ℓ-transfer emphasized

(t,α) High Q-value (+10-12 MeV)
Good reaction for proton pickup on all A at tandem energies
Poorly fit by DWBA due to momentum mismatch
Poor ℓ-transfer information

(t,t') Strong absorption reaction, isospin and spin of neutron.
May be compared to (^{3}He, ^{3}He') for isospin dependences in reaction

(t,p) Ideal two neutron stripping reaction for pairing studies, etc.

(t,^{3}He) Most straightforward isospin increasing charge exchange reaction
Used to study parents of giant resonances and neutron-rich nuclei

Figure 1. Summary of Triton properties and differential cross section

accurate spectroscopic factors and angular momentum transfer information. The (t,p) reaction is also well fit by these techniques and represents the simplest of the two neutron stripping reactions. The (t,α) reaction has several advantages as a proton pickup reaction principally in the high Q-value (≈ 12 MeV) and the high angular momenta excited. The former quality makes this reaction useful at typical Van de Graaff energies throughout the periodic table, whereas the competing reaction, (d,^{3}He), requires relatively high bombarding energies. Isospin properties of nuclear states may be investigated by comparisons of (t,t') and (^{3}He,^{3}He') and by the charge exchange reaction, (t,^{3}He). The latter has been used successfully to study the charge exchange mode of the giant M 1 mode[4].

From the above arguments regarding the usefulness of polarized beams and a triton beam, it is clear that a polarized triton beam can combine the advantages of the properties of both techniques. The development of a polarized triton beam at Los Alamos[5] now permits such an experimental program. Initial reaction studies with the polarized triton beam have been 1) ($\vec{t}$,α) studies of Pb and Zr nuclei[6] and a survey of rare earth nuclei[7], 2) ($\vec{t}$,p) reactions on spherical nuclei[8], to unnatural states[9], a study of the Ni isotopes [10] and a search for interference phenomena in the Pd-Te region[11], 3) a ($\vec{t}$,d) reaction on ^{58,64}Ni targets[12], 4) a (t,t') reaction on these same targets[13] and 5) a study of super-multiplet symmetry in the mass six system through the ^{9}Be($\vec{t}$,^{6}He) ^{6}Li reaction[14]. The present article discusses the significant aspects of these various reactions.

II. Experimental Aspects of the Polarized Triton Beam Studies

The polarized triton source developed by Hardekopf et al.[5] was used for the present studies. Beam currents averaging 75 nA and 0.75 polarization and with a spatial definition of 0.75 x 3 mm were used on targets for a Q3D spectrometer[15]. The spectrometer was operated at a solid angle of 14.3 msr and the reaction products were particle identified and spatially localized in a helically wound cathode proportional chamber on the focal plane[16]. The experimental resolution was generally determined by the target thickness which was usually chosen as a compromise between counting rate and optimal resolution. The thinnest targets produced 10 keV with more typical results being 15 - 18 keV.

An on-line computer controlled the complete measurement sequence at any given spectrometer angle. The computer measured the polarization of the beam and its direction then changed the direction after the initial run, again determining the polarization. Asymmetries were calculated automatically after this sequence using gates set on all interesting peaks in the initial run. Cross sections have been measured to a fraction of a μb using these techniques with running times less than one hour.

III. The $(\vec{t},\alpha)$ Reaction

The first (t,α) reactions were carried out on spherical nuclei with well established low lying single particle states. These, then, served as templates for establishing the spins of other levels higher in excitation or in nearby nuclei where previous experimental evidence was inadequate to give the total angular momentum. These cases also provide a comparison of DWBA predicted analyzing powers to the measured results. This comparison is quite useful in establishing the necessary optical model parameters for obtaining spins of nuclear states of different Q-value and masses from the original templates.

Results of the $^{208}Pb(\vec{t},\alpha)^{207}Tl$ and $^{90}Zr(\vec{t},\alpha)^{89}Y$ analyzing power studies are shown in Figs. 2 and 3 where they are compared to DWBA calculations[6]. In general, the fits are quite reasonable (the $g_{9/2}$ state of ^{89}Y is poorly fit) and a clear spin differentiation is noted. The analyzing powers are large and reasonably structured indicating the $(\vec{t},\alpha)$ reaction has excellent properties for total angular momentum measurements. As is seen above, the lead results may be extended over a large range of A with only small changes in shape.

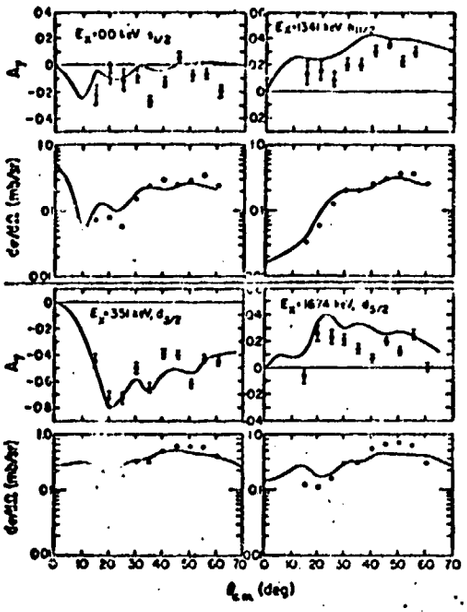

Figure 2. Analyzing powers and differential cross sections for the $^{208}Pb(\vec{t},\alpha)^{207}Tl$ reaction to single hole states. The solid lines are DW calculations.

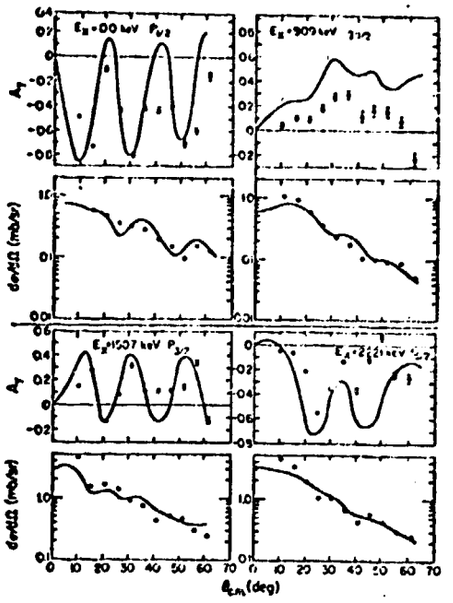

Figure 3. Analyzing powers for the $^{90}Zr(\vec{t},\alpha)\ ^{89}Y$ reaction. The solid lines are DW calculations.

This feature is exploited below in a study of the rare earth and actinide nuclei.

Extensive measurements covering 14 targets have been completed in the rare earth region[7,17] with targets ranging from ^{150}Sm up to ^{192}Os. Many of the neutron rich targets lead to completely new level schemes for the residual nuclei because of the difficulty of using other proton pickup reactions as mentioned above. Typical among these nuclei for which extensive new results have been obtained are ^{153}Pm, $^{157,159}Eu$, $^{167,169}Ho$ and $^{189,191}Re$. The large A rare earth nuclei may borrow most heavily from the lead template structure with these same orbitals predominating here except for certain Nilsson orbitals which drop rapdily such as the $9/2^-$.

At the lighter end of the rare earth region additional spins are noted. An example of the $^{154}Sm(\vec{t},\alpha)$ spectrum is noted in Fig. 4 where the large analyzing powers are immediately obvious in a comparison of the spin up and down spectra. Analyzing power and differential cross sections for the

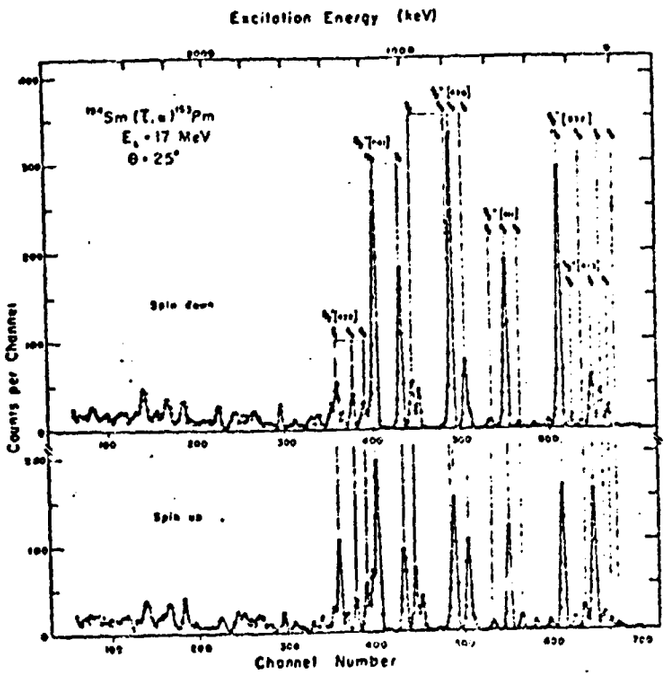

Figure 4. Spectrum of the $^{154}Sm(\vec{t},\alpha)$ ^{153}Pm reaction. Both spin configurations are shown.

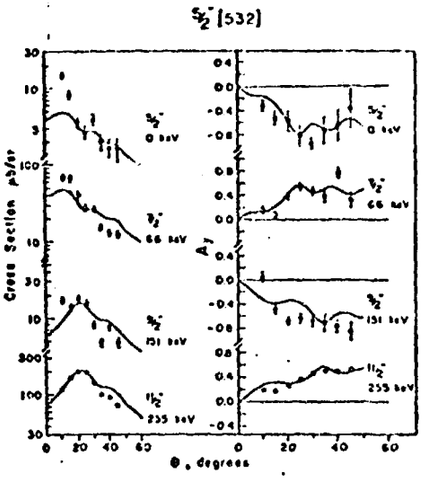

Figure 5. Analyzing powers and differential cross sections for the $^{154}Sm(\vec{t},\alpha)^{153}Pm$ reaction leading to the $5/2^-[532]$ band. The solid lines are DW calculations.

$5/2^-[523]$ band are shown in Fig. 5. The band originates in the $h_{11/2}$ orbital with the single particle strength for the $5/2^-$ and $7/2^-$ states coming up from the shell below. These latter states are poorly fit by DW calculations for the cross section but well fit for A_y. It is unclear if this is a coupled channel effect or a defect in the DW results.

There are a number of cases of serious conflict between DW calculations and the A_y measurements for states of known spin but which are weakly excited. Figure 6 contains several examples of these discrepancies. Here it is seen that the $7/2^+$ member of the $3/2^+[411]$ band is poorly fit by DW predictions in both ^{153}Pm and ^{165}Ho whereas this spin is well described for the $5/2^+[413]$ Nilsson orbital in ^{165}Ho. This latter state is relatively strong with a peak cross section of $\sim$ 120 μb/sr as compared to the anomalous shape states with $\sim$ 20 μb/sr. The differential cross section on these latter states are also poorly fit so it is difficult to state whether the observed cross section is in agreement with single step Nilsson model predictions. These states, and

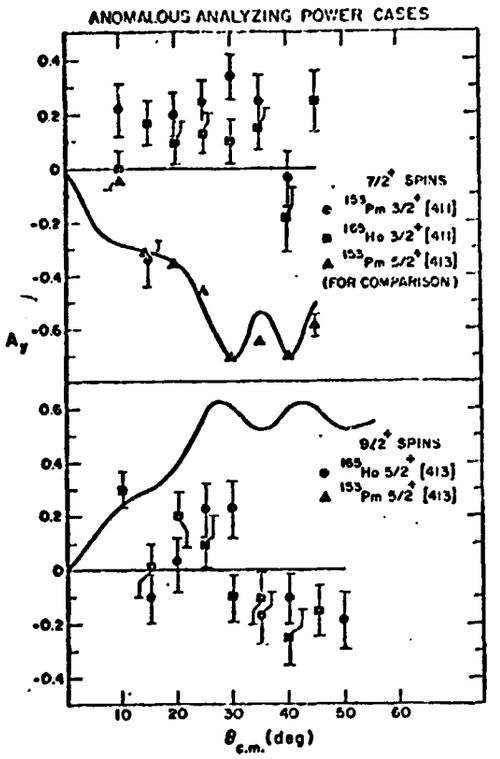

Figure 6. Examples of anomalous analyzing powers in the $(\vec{t},\alpha)$ reaction.

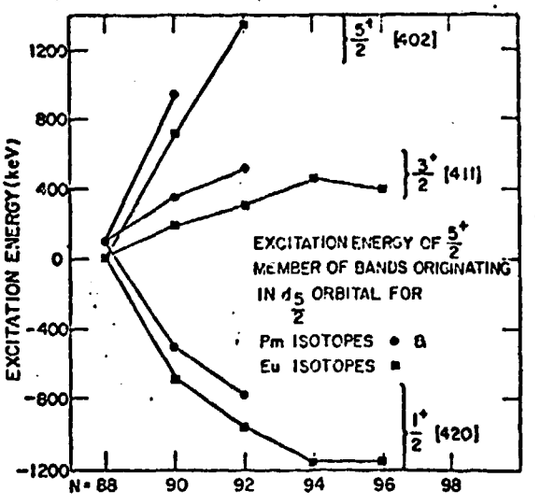

Figure 7. Systematic behavior of Nilsson levels originating in the $d_{5/2}$ shell model orbital as a function of neutron number.

there are other $7/2^+$ and $9/2^+$ states throughout the rare earth nuclei examined, are clear examples of coupled channel effects and warrant a serious effort by nuclear reaction theorists to explain their behavior. Presumably, the principal multistep channel would be through the strong inelastic quadrupole state followed by a single proton transfer to one of the strong Nilsson orbitals.

An example of the systematic behavior of certain Nilsson levels as prepared by D. Burke is shown in Figure 7. Here proton states originating in the $d_{5/2}$ shell model orbital are traced as a function of neutron number for Pm and Eu isotopes. It is clear from this that the neutrons play the major deformation inducing role as both elements follow similar patterns when crossing the transition region at N = 90. These are the only three Nilsson orbitals originating from the $d_{5/2}$ orbital. It is planned to extend these systematics throughout the deformed region.

A final example of the use of the $(\vec{t},\alpha)$ reaction in determining nuclear level schemes is in the actinide region where the reactions ^{234}U and ^{244}Pu

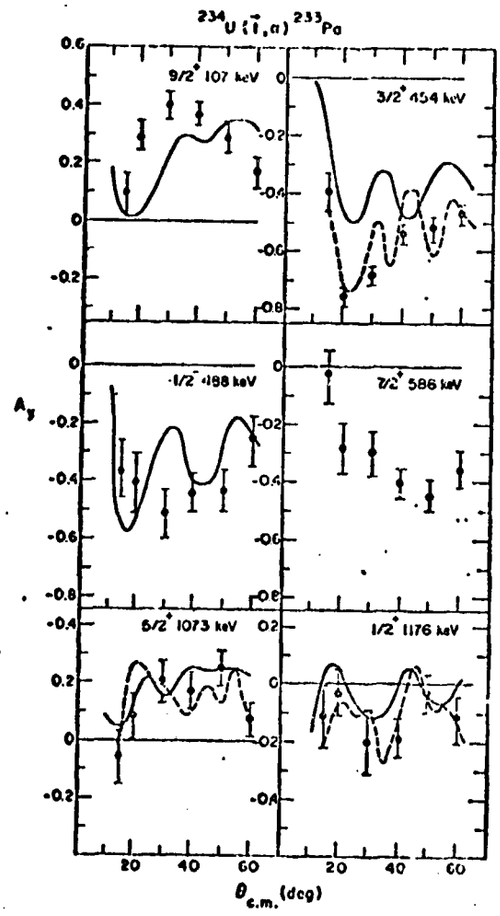

Figure 8. Analyzing powers for several levels seen in the $^{234}U(\vec{t},\alpha)^{233}Pa$ reaction. The solid lines are DW calculations and the dashed lines are empirical fits to the lead results of Figure 2.

$(\vec{t},\alpha)$ to ^{233}Pu and ^{243}Np has been completed[18]. This region is more complex than the rare earth's because of a higher level density, lower cross sections, and a larger degeneracy in possible spin values. Figure 8 is an example of a selection of analyzing powers to various states in ^{233}Pa. The data are compared to DW calculations and empirical shapes from ^{208}Pb $(\vec{t},\alpha)$, the latter assuming that these arise from a crossing of the Z = 82 shell due to deformation. Reasonable success is seen in describing these states and the technique has been used to investigate the previously unknown nucleus ^{243}Np.

IV. The $(\vec{t},d)$ Reaction

As mentioned above, the (t,d) reaction has a number of excellent attributes for the measurement of neutron single particle states and in some cases offers advantages over the (d,p) reaction. In particular, the (t,d) reaction is well described by DW calculations, has an excellent diffractive structure in light to medium weight nuclei and excites higher angular momentum states more strongly than the $(\vec{d},p)$ reaction. Recently, we have examined the $(\vec{t},d)$ reaction on targets of $^{58,64}Ni$ to investigate the usefulness of measurements of A_y in obtaining nuclear spins[12]. The resulting A_y values for the p and f orbitals are shown in Figure 9 where they are compared to DW calculations. Reasonable agreement is found with these calculations

except for the $7/2^-$ state which represents only a small fraction of the $f_{7/2}$ strength approximately seven MeV removed from the single particle centroid. These data show rapid oscillations with clear spin determinations over the range of angles examined. It may be pointed out that this angular range is only one half of that required to obtain similar information in the $(\vec{d},p)$ reaction at comparable energies; the period of the $(\vec{t},d)$ A_y values is 20° versus 50° for the $(\vec{d},p)$. This makes the experimental measurements somewhat simpler. In general, the A_y structure is sufficient to obtain j and ℓ, the exception being very weak states such as the $7/2^-$ which may well have multiple step contributions occurring. In all cases in ^{59}Ni, the analysis of A_y measurements agreed with known spin values.

In the ^{65}Ni situation, there are a number of spins unknown in the low lying levels and several additional ambiguities exist. Initial (d,p) data[19] had suggested that a major fraction of the $9/2^+$ strength comes rapidly down in excitation energy as a function of N; however, recent subcoulomb stripping data disputes this[20]. This rapid lowering of the $g_{9/2}$ strength is thought to be associated with the onset of a shape transition between N = 40 and 42 and

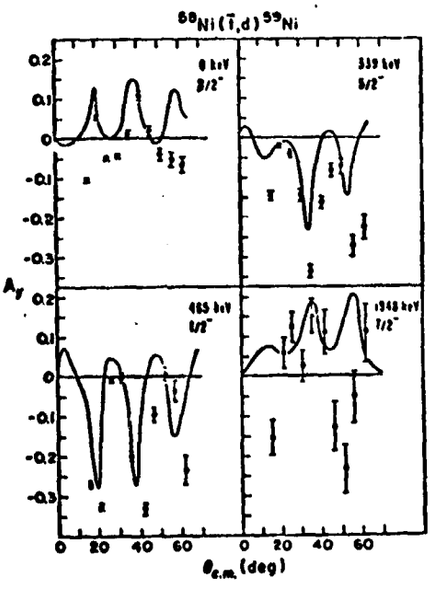

Figure 9. Analyzing powers for the ^{58}Ni($\vec{t}$,d)^{59}Ni reaction leading to p and f orbitals. The solid lines are DW calculations.

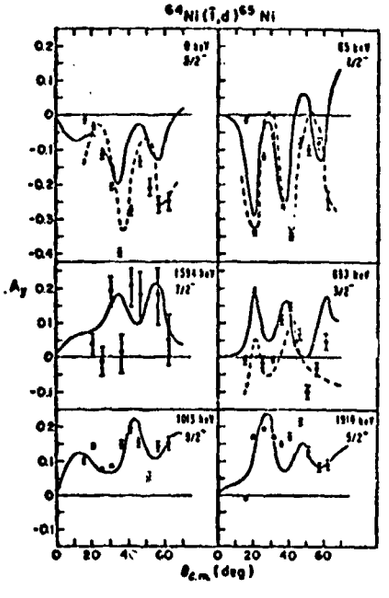

Figure 10. Analyzing powers for the ^{64}Ni($\vec{t}$,d)^{65}Ni reaction for a number of states. The solid lines are DW calculations and the dashed lines empirical to the data of Figure 9.

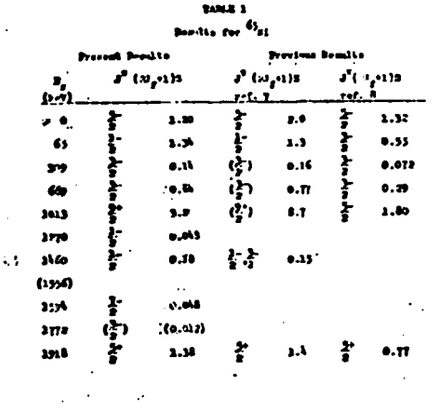

Figure 11. A summary of $^{64}Ni(\vec{t},d)^{65}Ni$ results compared to previous results.

the recent results suggesting it does not come down would alter this concept radically.

Figure 10 contains the A_y values for six levels in ^{65}Ni. The data are compared to DW calculations and empirical results from the ^{59}Ni case which was shown in Figure 9. Aside from anticipated kinematic shifts the empirical shapes quite adequately describe a number of states in ^{65}Ni permitting definitive spin assignments. The DW results corroborate this interpretation. The level at 1013 keV does not fit either a p or f orbital both in analyzing power or differential cross section (not shown here). The $9/2^+$ assignment suggested by Fulmer and McCarthy[19], however, does agree well with these measurements and suggests about 1/3 of the $g_{9/2}$ strength has dropped to this energy. The level at 1918 keV also is fit best by a $5/2^+$ assignment with about 25% of the strength at this energy. This strongly indicates that the filling neutron shell is inducing a nuclear deformation which brings a significant fraction of the $d_{5/2}$ orbital across the shell gap of $\sim$ 5 MeV which should exist between the f-p shell and the $d_{5/2}$ shell. Figure 11 summarizes the ^{65}Ni results and it can be seen that the current $(\vec{t},d)$ data permits the assignment of ten spin values below 2 MeV. The recent subcoulomb (d,p) results also seem to be in error in assigning spins of $3/2^-$ and $5/2^-$ to the 65 and 1013 keV levels respectively. The A_y values observed for the $(\vec{t},d)$ reaction at this energy give sharp diffractive structure and unambiguous spin values for spins up through $9/2^+$ and of reasonable spectroscopic strength (> .02).

V. The $(\vec{t},p)$ Reaction

The (t,p) reaction has long been an important tool in the study of nuclear pairing phenomena in spite of a rather complex reaction mechanism. Empirical analysis of a wide range of data by DW techniques using microscopic form factors[21] has shown that consistent spectroscopic information may be obtained[22]. On the other hand, it is known that the reaction mechanism is complex with appreciable two step processes occurring although, in the majority of cases, these represent a constant fraction of the direct contribution

and thus are folded into the empirical normalization. Except for strongly deformed nuclei or very weak direct transition strength, the shape of the differential cross section is not very influenced by two-step contributions and the influence of such effects must be felt only in the magnitude and thus unfolded from the empirical normalization.

As discussed above, a measurement of A_y for the reaction of interest increases the sensitivity of the experiment to details of the nuclear structure. In the case of two nucleon transfer reactions this aspect may be used for a further study of the influence of two step processes. A series of studies involving the $(\vec{t},p)$ reaction has been carried out for this purpose.

Figures 12 and 13 show several results for spherical nuclei and reasonably strong states using the ^{90}Zr, $^{208}Pb(t,p)$ reactions as examples[8]. In the Zr case it is worth noting that similarity between A_y results for the two 0^+ states as well as the three 2^+ states. This similarity is significant in view of the fact that these states have substantially different wave functions; the 935 keV is dominated by $d_{5/2}^2$ (0.910 amplitude) whereas the 2070 keV is a mixture of $d_{5/2}^2$ and $d_{5/1}s_{1/2}$ (-0.32 and 0.52 amplitudes). Wave functions containing these amplitudes have been used to provide a reasonable description of the (t,p) cross sections[23]. We shall return to the Zr case below where the similarity in A_y results will have significant meaning.

The lead results of Figure 13 are reasonably well described by the DWBA for lower L-transfers as was the Zr case. The larger L-transfers show increasing deviation of the A_y data from polarization predictions and this is not understood. Certainly, there is a decreased probability for inelastic channels contributing to the reaction as compared to the low-lying 2^+ and 4^+ states. The addition of consecutive particle transfer on a two step process may improve the fit to these data although this has not been tried. It would be a nice success for such theories to improve the description of A_y for 6^+ and 8^+ states in particular as these are relatively pure $g_{9/2})_J^2$ states.

The nickel isotopes offer an example of somewhat more collective behavior although still not well deformed. As mentioned above, the rapid descent as a function of neutron number of the $g_{9/2}$ and $d_{5/2}$ orbitals is an indication of at least a tendency towards deformation and the resulting increased collectivity. Previous examination of this region for coupled channel effects involving excitation of unnatural parity states which are forbidden in a direct process has been reported by Boyd, Alford et al.[9]. Such data show a large sensitivity to the nuclear structure of the excited states. More recently

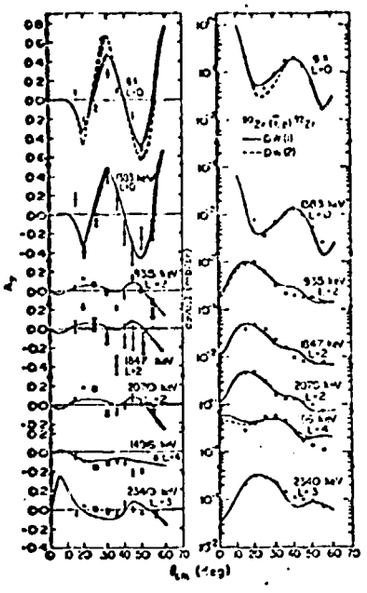

Figure 12. Analyzing powers for the $^{90}Zr(\vec{t},p)^{92}Zr$ reaction. The solid curves are DW calculations.

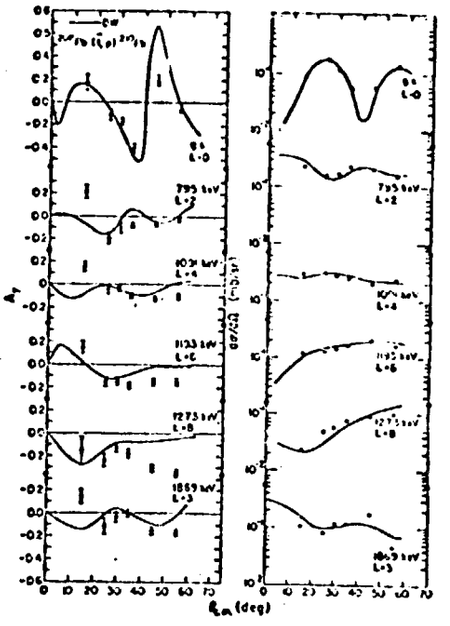

Figure 13. analyzing powers for the $^{208}Pb(\vec{t},p)^{210}Pb$ reaction. The solid curves are DW calculations.

Alford, Boyd et al.[10] have measured A_y for the natural parity states and some of these results are shown in Figure 14. A judicious choice of optical model parameters permits an excellent fit by single step DW calculation to the ground state transitions as seen in this figure. However, the 2^+ states are not as well described with a phase difference between data and calculation noted as well as a disparity in magnitude at back angles. This disparity becomes worse with increasing neutron number; the collectivity of this 2^+ is also increasing with neutron number. The data can be better described by allowing consecutive particle transfer through the (t,d) (d,p) channel as the calculation labeled CCBA in Figure 15 indicates. However, the more expected inelastic channel had no effect on the shape of the analyzing power. Again the A_y shapes indicate a great sensitivity to nuclear structure and the more complex CCBA calculations are able to describe the A_y features. In this case the calculation which best describes the data was not the expected one.

Quite recently Yagi et al.[3] have utilized this sensitivity of the two nuclear transfer A_y values to explore the effects of the filling of the neutron shell between N = 50 and 82. They have observed a change in the sign of the analyzing power for the $(\vec{p},t)$ reaction for the lowest 2^+ which occurs -

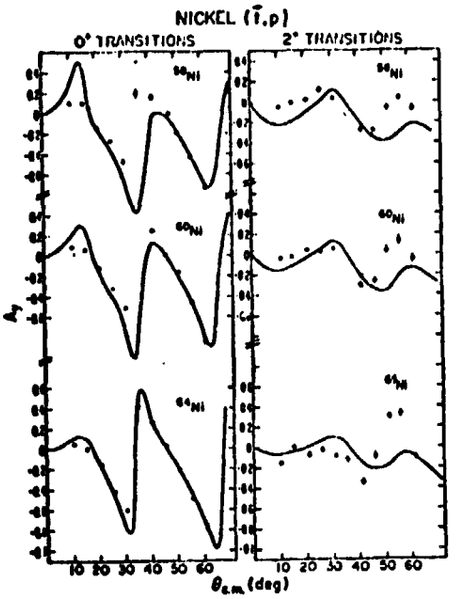

Figure 14. Analyzing powers for the $^{58,60,64}Ni(\vec{t},p)$ reaction to g.s. and 2^+ states. The solid curves are DW calculations and the dashed curves are CCBA calculations.

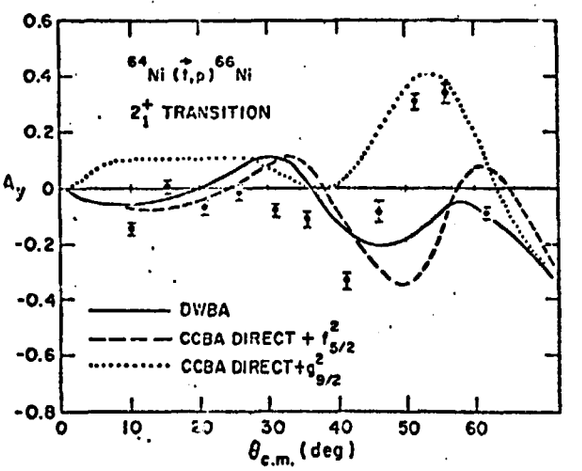

Figure 15. Comparison of CCBA and DWBA calculations to the A_y values for the $^{64}Ni(\vec{t},p)^{66}Ni(2_1^+)$ transition.

between the Pd and Te nuclei. They interpret this result as an interference between the direct transfer and the two step channel through the inelastic excitation of the 2^+. Because of the filling neutron shell, the importance of the forward and backward amplitudes changes, as do the U and V factors, between Pd and Te and the interference goes from constructive to destructive. These authors[3] suggest that this effect is responsible completely for the experimental A_y sign change.

The inverse reaction, $(\vec{t},p)$, has now also been employed on the Pd and Te nuclei and combined with the Zr results discussed above. Results of A_y for the ground state and lowest 2^+ for targets of ^{106}Pd and ^{126}Te are shown in Figure 16. Also shown are single step DW calculations employing a $d_{5/2}^2$ form factor and standard optical model potentials (a different potential family then employed in reference[8] is used here). It is worth noting that the 2^+ cross sections decrease with increasing neutron number being in the ratio of 1.0:0.0[illegible]:0.015 for the ^{90}Zr, ^{106}Pd and ^{126}Te targets respectively. This is opposite to the trend in the (p,t) data and perhaps indicating the relative roles of orbitals above and below the Fermi surface. The A_y data show sharp

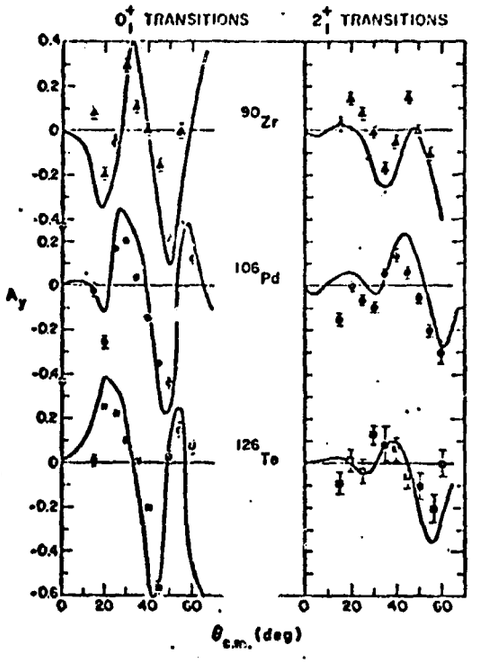

Figure 16. Analyzing powers for the ^{90}Zr, ^{106}Pd, $^{126}Te(\vec{t},p)$ reaction leading to the g.s and $2,^+$ states. The solid curves are DW calculations.

diffraction structure for the g.s. transitions which are typical of L = 0 transfers. The DW fit to these data show an extreme sensitivity to the proton optical potential and the real well depth has been adjusted by + 3 MeV in all three cases to give the correct period. The L = 0 data are well reproduced by these DW fits even in the details of shifting minimum with mass and the gradual dissappearance of the forward angle minimum. The DW calculations are averaged over the Q3D solid angle. These results illustrate that single step DW results quite adequately describe the dominant $(\vec{t},p)$ transitions.

The transitions to the 2^+ states show a rapidly changing structure for A_y as a function of increasing neutron number. However, contrary to the (p,t) results, the single step DW calculation reproduces most of these variations. Thus in the case of the $(\vec{t},p)$ A_y data the interference between direct and inelastic channels is not evident. Naively, one would have expected an opposite effect for the (t,p) from that of the (p,t). However, one must take into account the relative direct two-nucleon transition strength of the various orbitals. The (p,t) reaction has access to the $s_{1/2}$ orbital which lies below the Fermi surface near A = 110 + 120 and carries a large intrinsic direct strength. Only a small fraction of this strength is available to the (t,p) reaction except at smaller A near ^{90}Zr. This could explain the larger discrepancy with the DW calculation seen here although here the 2^+ is not as collective. It remains yet to do the complete rpa calculation with coupled channel calculation as described in reference[3] for the (t,p) reaction to see if the above conjectures regarding the importance of various orbitals is correct.

VI. Conclusions

Although the polarized triton beam has been in existence for only a short time, it has proved to be extremely successful in the study of nuclear phenomena. A considerable wealth of data now exists on proton hole states through the $(\vec{t},\alpha)$ reaction and similar results are now being obtained for neutron particle states from the $(\vec{t},d)$ reaction. The $(\vec{t},p)$ reaction is also being used successfully to provide detailed checks on reaction mechanisms and as a sensitive check on nuclear wave functions. Additional measurements of the $(\vec{t},t')$ and $(\vec{t},{}^3He)$ reaction are also underway.

The author is grateful to P. Alford, R. Boyd, R. Brown, D. Burke, J. Cizewski, D. Hanson, R. Hardekopf, G. Lovhoiden, E. Sugarbaker and J. Sunier for excellent collaborations in various aspects of this program. This work has been performed under the auspices of the U.S. Department of Energy.

References

1. e.g. see Proceedings of 4th Int. Sym. on Polarization Phenomena in Nuclear Reactions, eds., W. Grüebler and V. König, Zurich 1975 - Birkhaüser Verlag Bassel 1976, p. 229 and p. 647ff.
2. e.g. ibid, p. 333, p. 719ff, p. 763ff.
3. K. Yagi, S. Kunori, Y. Aoki, Y. Higashi, J. Sanada and Y. Tagishi, Phys. Rev. Letts. 40, 161 (1978).
4. E. R. Flynn and J. D. Garrett, Phys. Rev. Lett. 29, 1748 (1972).
5. R. A. Hardekopf, G. G. Ohlsen, R. V. Poore and N. Jarmie, Phys. Rev. C13, 2127 (1976).
6. E. R. Flynn, R. A. Hardekopf, J. D. Sherman and J. P. Coffin, Phys. Rev. Lett. 36, 79 (1976).
   E. R. Flynn, R. A. Hardekopf, J. D. Sherman, J. W. Sunier and J. P. Coffin, Nucl. Phys. A279, 394 (1977).
7. For example see C. R. Hirning, D. G. Burke, E. R. Flynn, J. W. Sunier, P. A. Schmelzbach and R. F. Haglund, Jr., Nucl Phys. A287, 24 (1977).
8. E. R. Flynn, R. A. Hardekopf, J. D. Sherman and J. W. Sunier, Phys. Letts. 61B, 433 (1976).
9. R. N. Boyd, W. P. Alford, E. R. Flynn and R. A. Hardekopf, Phys. Rev. C15, 1160 (1977).
10. W. P. Alford, R. N. Boyd, S. Sugarbaker, D. L. Hanson and E. R. Flynn, to be published.

11. W. P. Alford, R. E. Brown, J. Cizewski, E. R. Flynn, D. L. Hanson, E. Sugarbaker and J. W. Sunier, to be published.
12. E. R. Flynn, R. E. Brown, F. D. Correll, D. L. Hanson and R. A. Hardekopf, to be published.
13. R. E. Brown, F. D. Correll, E. R. Flynn, D. L. hanson and R. A. Hardekopf, to be published.
14. E. R. Flynn, R. E. Brown, R. F. Haglund, Jr., R. A. Hardekopf, P. A. Schmelzbach, J. W. Sunier and W. von Oertzen, to be published.
15. E. R. Flynn, S. D. Orbesen, J. D. Sherman, J. W. Sunier and R. W. Woods, Nucl. instr. and Meth. 128, 35 (1975).
16. S. D. Orbesen, J. D. Sherman and E. R. Flynn, Los Alamos report LA-6271-MS.
17. D. G. Burke, G. Lovhoiden, E. R. Flynn and J. W. Sunier, a series of papers to be published.
18. E. R. Flynn, D. L. Hanson and R. A. Hardekopf, Phys. Rev., to be published.
19. R. H. Fulmer and A. L. McCarthy, Phys. Rev. 131, 2133 (1965).
20. P. Staub, E. Baumgartner, J. Saladin, H. Schar and D. Trautman, HeV. Phys. Acta. 50, 9 (1977).
21. P. D. Kunz, U. of Colorado code DWUCK, unpublished and B. F. Bayman and A. Kallio, Phys. Rev. 156, 1121 (1967).
22. E. R. Flynn and Ole Hansen, Phys. Letts. 31B, 135 (1970).
23. E. R. Flynn, J. G. Beery and A. G. Blair, Nucl. Phys. A218, 285 (1974).